Seasonality of $U^{K'}_{37}$ temperature estimates as inferred from sediment trap data

Antoni Rosell-Melé [a,b*] and Fredrick G. Prahl [c]
[a]ICREA, Pg. Lluís Companys 23, 08010 Barcelona, Catalonia, Spain
[b]Institut de Ciència i Tecnologia Ambientals and Department of Geography, Universitat Autònoma de Barcelona, 08193 Bellaterra, Catalonia, Spain
[c]College of Earth, Ocean and Atmospheric Sciences, Oregon State University, Corvallis, USA 97331-5504

* Corresponding author
Institute of Environmental Science and Technology
Autonomous University of Barcelona
Edifici Cn - Campus UAB, 08193 Bellaterra, Catalonia (Spain)
Tel.: +34 93 581 3583
Fax: +34 93 581 3331

Abstract

The seasonality of sea surface temperatures (SST) estimated from the alkenone- $U^{K'}_{37}$ index has been a debated issue since the development of the proxy. Using a compilation of sediment trap time series data from 34 sampling locations, we show that the seasonality of maximum alkenone flux in sediment traps varies markedly across the oceans, depending not only on latitude and light availability but also on local oceanographic conditions. The seasonality of the alkenone flux to sediments may also be shaped by the complexity of sedimentation processes and a consistent, globally applicable, seasonal pattern is not apparent. Nevertheless, $U^{K'}_{37}$ values display a world ocean scale correlation with mean annual SSTs (0 m) that closely resembles the standard calibration equation now established for modern surface sediment records. Thus, with a few notable exceptions at oceanographic locations proximate to major hydrographic fronts, it can be concluded that the integrated sedimentation patterns for $U^{K'}_{37}$ measured in sediment trap time series provide a measure of annual mean SST.

1. Introduction

C_{37-39} alkenones are lipids exclusively synthesized by a restricted group of Haptophyte algae (de Leeuw et al., 1980; Volkman et al., 1980). The proportion of di-unsaturated to tri-unsaturated C_{37} alkenones, expressed as the $U^{K'}_{37}$ index, correlates linearly with algal growth temperature (Conte et al., 1998a; Prahl et al., 1988; Prahl and Wakeham, 1987). Thus, sea surface temperature (SST) is now the primary variable considered in the paleoceanographic interpretation of the sedimentary $U^{K'}_{37}$ values (Fischer et al., 2010). However, an interpretation of how seasonality in sedimentary flux impacts the geological record for the $U^{K'}_{37}$-temperature signal is a much more debatable issue. Given marked seasonality in the abundance of primary producers and the link between primary production and SST (e.g. Behrenfeld et al., 2006), others have postulated that the biomarker signal recorded in sediments reflects the season of maximum alkenone production and export from the surface ocean – generally argued to be within the spring to summer time frame (Brassell, 1993; Brassell et al., 1986; Conte et al., 1992; Leduc et al., 2010; Martínez-Garcia et al., 2009; Schneider et al., 2010; Sikes et al., 2002).

However, this interpretation seems in conflict with the results from the global core-top calibration of U^{K}_{37}', where the best fit is obtained with annual mean SSTs (Conte et al., 2006; Müller et al., 1998b). The linear equation obtained is statistically indistinguishable from the first published calibration based on experimental study of a single culture of *Emiliania huxleyi* (Prahl et al., 1988), the most ubiquitous modern coccolithophorid. This finding reinforced the validity for wide use of a single, empirical equation to estimate past SSTs. Nonetheless, there remains a lack of understanding of key processes that lead to the accumulation of alkenones in sediments, among which include the depth and seasonality of export from the euphotic zone as well as the relative importance of complications caused by lateral advection of signals (e.g. Bendle and Rosell-Melé, 2004; Benthien and Muller, 2000; Giraud, 2006; Prahl et al., 2010; Rühlemann and Butzin, 2006).

To account for seasonal bias, various others have tried to redefine the global core-top calibration by weighting it with surface ocean primary productivity or by defining new indices based on integrated production temperatures. However, the resultant equations did not reduce the errors of the estimates sufficiently (Conte and Eglinton, 1993; Conte et al., 2006; Conte et al., 1998b; Giraud, 2006; Sonzogni et al., 1997). Despite the uncertainties of alkenone thermometry, $U^{K'}_{37}$ estimates of SST often match those derived from other proxy approaches within the respective uncertainty brackets (Bard, 2001; Waelbroeck et al., 2009). When divergence of multiproxy estimates is encountered, however, the cause is often ascribed to the seasonal bias of alkenone export production, or even more complex to assess, a change in such seasonality through time (e.g. Chapman et al., 1996; de Vernal et al., 2006; Haug et al., 2005; Leduc et al., 2010; Schneider et al., 2010).

We now appraise the issue of seasonality encoded in the sedimentary U^{K}_{37}’ signals through analysis of a compilation of alkenones flux data from study of sediment trap time series over a broad oceanographic range. These data sets have been examined specifically to seek objective answers to three key questions:

1) Is there a latitudinal dependence in the seasonal timing of maximum alkenone flux through the water column?
2) If so, is perceived seasonality of alkenone export from production in surface waters transferred coherently to sediments?
3) Does the $U^{K'}_{37}$ temperature signal of the annually-integrated alkenone flux correspond to the annual SST or is there as seasonal bias?

2. Description of the data sets and methods

We have compiled alkenone flux data from sediment trap time series studies conducted at 34 locations spanning time frames from months up to 5 years (Table 1 and Fig. 1). The distribution of observations is very uneven globally, with most (90%) of the studies done in the northern hemisphere – 2/3 in the Pacific Ocean and 1/4 in the Atlantic Ocean. Only two studies were done in the Southern Ocean (Indian and Pacific Ocean Sectors) and one in the Indian Ocean (Arabian Sea). The northwest Pacific (including the Okhotsk and Japan/East seas) is the area of the world that has been most thoroughly examined, accounting for 1/3 of the total sediment trap deployments. From a global perspective, most study sites were located on, or relatively near the continental shelf, although more than half of them can be considered pelagic settings as deployments were made at ≥1000 m water depth, or were located near remote islands in the central Pacific (Hawaii archipelago) or Indian Ocean (Kerguelen Island). Several studies in the compilation were done in marginal seas: Mediterranean Sea (1), Japan/East Sea (2), Okhotsk Sea (2), Cariaco Basin (1) and Gulf of California (1). Only three studies were done in subpolar environments – both subarctic (1) and subantarctic (2) waters. And, six were in the tropics between 0 and 30°N, with one site located on the equator. On a hemispheric basis, the average latitudinal or longitudinal spread of the deployments is quite comprehensive to the north of the equator, but spotty to the south. We use a compilation of polar plots (Fig. 2) to illustrate using time series data from the shallowest sampling depth at each site how the intensity of seasonal patterns varies throughout the global ocean.

Most of the sediment trap time series studies report values for $U^{K'}_{37}$, total alkenone (K37s) flux and deployment time on a temporal basis. Therefore, we are able to calculate the flux weighted $\bar{U}^{K'}_{37}$ for the total period of the trap deployment at each site using the formula:

The terms in this equation are: the alkenone unsaturation index ($U^{K'}_{37i}$), the mass flux of K37s ( ), and the time interval (for sampling in each sediment trap cup. varied from a few days to several months (depending on the study) but was commonly 0.5 to 1 month. We compare the data obtained to mean annual surface (0 m) water temperature values extracted from the 2001World Ocean Atlas (http://odv.awi.de/en/data/ocean/) (Fig. 3A) and to $U^{K'}_{37}$ values measured in surface sediment underlying the trap site for all case where such information is also available (Fig 3B). The use of a different version of the Atlas is unlikely to affect the final outcome of the study given that the use of different versions in the literature yields comparable results (e.g. Conte et al., 2006; Müller et al., 1998b), and we could find no significant difference in our evaluation of the various versions.

3. Discussion

3.1. Timing of fluxes

The magnitude of K37s fluxes varies markedly across the oceans (Table 1 and Fig. 1A). Lowest values were measured in the Japan Sea ($\leq 10^{-2}$ μg m^{-2} d^{-1}) followed by sites at high northern latitudes in the open Pacific and the Atlantic Oceans, high southern latitudes in the open Indian Ocean and in the oligotrophic Mediterranean Sea (0.1-1 μg m^{-2} d^{-1}). Highest fluxes (up to ~35 μg m^{-2} d^{-1}) are noted along continental margins (east of New Zealand and Japan fall in this category), proximate to upwelling regions (Cariaco Basin, NW Africa) and in the Gulf of California.

Most studies show that the highest annual K37s flux is generally associated with either a single export event or bi-seasonal export events (Fig. 2, Table 1). Bi-seasonal export events have been reported in the subtropical and subpolar northern Atlantic (Thomsen et al., 1998; Waniek et al., 2005), the Mediterranean (Ternois et al., 1996) and Japan/East seas (Lee et al., 2011), the Southern Ocean-Indian Sector (Ternois et al., 1998), and the subtropical southwest Pacific (Sikes et al., 2005). However, export events are not always confined to a short time duration. In some cases, they lasted for several months, even extending into multiple seasons. For instance, one such prolonged high flux event (10-100 times higher values during [8–21 μg m^{-2} d^{-1}] than before and after [<1μg m^{-2} d^{-1}]) in subantarctic waters in the western South Pacific began in August (late austral winter), peaked in November (late austral spring), and ended in December (early austral summer) (Sikes et al., 2005). Some sites in the tropics (between 30° north and 30° south) or near the equator displayed no marked seasonality, and high K37s flux occurred under seemingly different circumstances in different months of the year. Multiyear time series for the Cariaco and Santa Barbara basins, the Gulf of California and the upwelling zone off Cape Blanc (Goni et al., 2004; Goñi et al., 2003; Goñi et al., 2001; Müller and Fischer, 2001) showed random variability in the measured K37s flux throughout the year and large interannual differences in absolute magnitude. At these sites, peak values occurred at different times than those of organic carbon and biogenic silica, an observation also made in the western equatorial Pacific where multiple high K37s fluxes occurred without evidence of a distinct seasonal pattern (Harada et al., 2001). Elsewhere, apparent non-seasonal variability in K37s flux was reported for the Sargasso Sea (not shown in Fig. 1A due to the short sampling period; Conte et al., 2003; Conte et al., 1998b), where high values occurred erratically in boreal winter and were decoupled with the annual phytoplankton spring bloom when highest organic carbon fluxes were measured. However, in the Arabian Sea, K37s flux maximized during the intermonsoon to monsoon transition period (Prahl et al., 2000). And at Station ALOHA, located just north of Hawaii in the oligotrophic North Pacific subtropical gyre, K37s flux varied widely with conspicuous maxima occurring bi-seasonally, i.e. during both a period of weak vertical mixing at the onset of winter and a period of strong stratification in summer (Prahl et al., 2005).

Acknowledging the limited spatial coverage of the compilation, Fig. 2 shows that no straightforward relationship exists between latitude and the timing or season(s) of the peak K37s flux. In fact, the period of highest values can vary for a similar latitudinal band. For example, a single export event occurred during spring transition at three locations along an offshore transect in the temperate NE Pacific and at a single location in the NE Atlantic off the Gulf of Biscay, while export events occurring both in spring/summer and autumn appear common in the Gulf of Maine, the Mediterranean Sea, the Norwegian Sea, the Sea of Okhotsk and a range of other sites in the NW Pacific (Table 1). Elsewhere in the NE Atlantic and the Mediterranean Sea, peak K37s flux occurred in winter or autumn, respectively, with secondary events in spring .

All available investigations show that K37s flux declines with water column depth, and often quite significantly (Table 1). The observed magnitude of attenuation with depth differs between sites. Furthermore, these records show that the marked seasonality in flux observed in some shallow traps can be lost with depth (Goñi et al., 2003; Harada et al., 2001; Lee et al., 2011; Müller and Fischer, 2001; Prahl et al., 2000; Sawada et al., 1998; Seki et al., 2007; Thomsen et al., 1998; Yamamoto et al., 2007). Notably, the magnitude of attenuation is higher during the period of maximum K37s flux than during less productive times. As a result, a higher proportion of the alkenone signal from the surface reaches a given depth during the lower productivity periods (Harada et al., 2001; Lee et al., 2011; Sawada et al., 1998; Thomsen et al., 1998; Yamamoto et al., 2007). However, this phenomenon of time dependant, differential flux attenuation with depth is not reported universally. In the upwelling region off Cape Blanc, the relative temporal flux pattern was similar in the same time periods at two depth levels, i.e., during February, from May to June, and in August, even though the trap sampling horizons were separated vertically by more than 2000 meters (Müller and Fischer, 2001).

In summary, there is no single seasonal pattern that describes alkenone flux to the seabed in the world ocean. Furthermore, the pattern observed for a given location can depend upon local factors, such as the depth in the water column where the measurements are made.

3.2. $U^{K'}_{37}$ in the sediment fluxes

The seasonal change of $U^{K'}_{37}$ values in sediment trap materials tracked the variability of the K37s flux in quite a few instances (Goni et al., 2004; Goñi et al., 2003; Goñi et al., 2001; Müller and Fischer, 2001; Prahl et al., 2000; Sawada et al., 1998; Seki et al., 2007; Sikes et al., 2005; Ternois et al., 1998; Yamamoto et al., 2007). But, in a number of cases, seasonal variability in $U^{K'}_{37}$ values was decoupled from the variability in K37s flux, and the $U^{K'}_{37}$-derived temperature estimates did not match overlaying SSTs (Conte et al., 1998b; Goñi et al., 2001; Harada et al., 2001; Harada et al., 2006; Prahl et al., 1993; Sikes et al., 2005; Yamamoto et al., 2007). For instance, in three NE Pacific sediment trap time series, which each displayed a pronounced peak in K37s flux during the spring transition (Prahl et al., 1993), $U^{K'}_{37}$ values were remarkably uniform throughout the time series, except during the high flux event. At that time, $U^{K'}_{37}$ values encoded a conspicuously “colder” signal than SST. And, for the most offshore location, $U^{K'}_{37}$ values corresponded with SST in winter but with that measured at the depth of the subsurface chlorophyll maximum prevalent during summer stratification. At other oceanographic sites, $U^{K'}_{37}$ estimates may reflect bias from advected or resuspended alkenones rather than the local seasonal pattern of export production from overlying surface waters (Harada et al., 2006; Prahl et al., 2001; Rosell-Melé et al., 2000; Sawada et al., 1998; Thomsen et al., 1998). In the case of some sediment trap time series, comparison of temperature estimates derived from $U^{K'}_{37}$ measurements in surface sediment with those from sediment trap data and/or suspended particulate material collected from the euphotic zone suggests that the record preserved in the sediment deposit reflects the seasonal signal of the peak K37s flux (Prahl et al., 2001; Seki et al., 2007). In others, however, the annual estimate for SST in the sediment trap time series matches the sediment record reasonably well (Goni et al., 2004; Goñi et al., 2003; Kawahata et al., 2009; Lee et al., 2011; Müller and Fischer, 2001; Prahl et al., 2005; Ternois et al., 1996).

To investigate further this issue, we calculated for the available data sets the flux weighted alkenone unsaturation index ($\bar{U}^{K'}_{37}$) for the complete period of each sediment trap time series deployment (Fig. 3). We note that, in the compiled data set, the average $U^{K'}_{37}$ for each trap is not significantly different from the calculated flux weighted index ($\bar{U}^{K'}_{37} = 1.03\ U^{K'}_{37} - 0.03$; $R^2 = 0.987$). With a few exceptions, $\bar{U}^{K'}_{37}$ values correlate linearly ($R^2 = 0.88$) with the annual mean SST (0 m) (Fig. 3A) obtained from the World Ocean Atlas (Conkright et al., 2002). The linear trend is quantitatively consistent with the $\bar{U}^{K'}_{37}$-annual mean SST calibration for global marine surface sediments (Müller et al., 1998b). Notably, $\bar{U}^{K'}_{37}$ values are generally concordant with $U^{K'}_{37}$ measured in underlying surface sediments at sediment trap sites where such data are available (Fig. 3B). The regression for sediment trap-derived $\bar{U}^{K'}_{37}$ data is, however, somewhat different from that obtained from an extensive global compilation of $U^{K'}_{37}$ measures made on suspended particulate materials from surface waters (Fig. 3A; Conte et al., 2006). The latter data set exhibits an apparent non-linear trend at colder temperatures, which is not mimicked by $\bar{U}^{K'}_{37}$ data below 20°C (Fig. 3A).

A clear explanation for this apparent lack of agreement is now not evident. Any explanation must take into consideration that suspended particulate material collected in surface waters represent alkenone-producing biomass. Such biomass is not equivalent with vertically transported alkenone-containing particulate materials collected in sediment traps or accumulating in surface sediments, which both are some reflection of export production, a very specific component of K37s productivity in surface waters.

3.3. Analysis of residuals

The data in Fig. 3 corroborate and further demonstrate that the sedimentary signatures of $U^{K'}_{37}$ are not conspicuously biased towards a particular high K37s flux season. In general, they are representative of annually integrated sedimentation processes as suggested from previous observations of $U^{K'}_{37}$ in water column particulates and sediments (e.g. Bentaleb et al., 2002; Conte et al., 2006; Doose et al., 1997; Herbert et al., 1998; Kienast et al., 2012; Müller et al., 1998b; Ohkouchi et al., 1999; Pelejero and Calvo, 2003; Pichon et al., 1998; Prahl et al., 2006; Rosell-Mele et al., 1995; Sikes et al., 1991; Sonzogni et al., 1997). Consequently, it seems justified to interpret downcore $U^{K'}_{37}$-SSTs as representative of annual mean SST at most oceanographic locations. But, it is also clear that some of the $\bar{U}^{K'}_{37}$ data in Fig. 3 fall well outside the general global trend. The most obvious 'outliers' encode a negative residual, a term defined by the difference between temperature estimated from $\bar{U}^{K'}_{37}$ using the global core top calibration equation (Müller et al., 1998a) and the annual mean SST obtained from the World Ocean Atlas (Conkright et al., 2002) (see Figs. 1B and 3).

Previously, we noted that some $U^{K'}_{37}$ trap values might be affected by inputs from advected or resuspended alkenones, as is likely the case for a sediment trap sampling location in the NE Atlantic and Norwegian seas (Rosell-Melé et al., 2000; Thomsen et al., 1998). However, a lateral advection artifact cannot be the explanation at all sediment trap sampling sites where large negative residuals are now evident. To some extent, local ecological or physiological processes in the water column conceivably impact the $U^{K'}_{37}$ signature and contribute to the significant deviation from the general trend (e.g. Prahl et al., 2010). Notably, the sites with large negative residuals (Fig. 1B) occurred at locations proximate to major fronts in SST and nutrients (Fig. 4). Clearly explaining how this oceanographic situation impinges the flux and composition of alkenones exported through sedimentation from surface waters at these specific sites is well beyond the scope of the data set available and primary purpose of this review paper. However, this yet observationally lean but nonetheless conspicuous finding supports the notion that non-random regional deviations from the global trend are possible and warranted further investigation (Prahl et al., 2010). It is paramount to develop independent means of analysis to identify where, when and why such deviations occur if oceanographic interpretation of sediment alkenone records of SST are to be refined (e.g. Haug et al., 2005; Prahl et al., 2006; Wolhowe et al., 2009).

4. Concluding remarks

The observed complexity in the seasonal patterns of alkenone export production to the deep sea is perhaps not surprising if viewed in context with the findings of compilations for particulate organic carbon flux in the global ocean (François et al., 2002; Honjo et al., 2008; Lutz et al., 2007). For example, in one of the largest published compilations of the latter to date, the authors argued that "c*omparison of production and flux variability shows a latitudinal dependant relationship. At lower-latitudes, seasonality of flux is typically greater than that of production, while at higher latitudes, seasonality of production is typically greater than that of flux. This reversal of variability may describe a biogeographic distinction in the controls of production-to-flux relationships*" (Lutz et al., 2007). The existing studies on alkenone flux do not yet allow us to provide such a succinct picture of the modern seasonality of K37s export from surface waters to the seabed and long-term sedimentary record. However, the perspective gained from the summary of all currently available, published results allow the three questions posed in the introduction to be addressed with significant confidence:

1) Alkenone flux to the deep sea is not necessarily coupled to patterns of bulk export primary productivity as gauged by organic carbon flux. Studies to date indicate that the seasonality of maximum K37s flux varies markedly across the oceans, depending on the characteristics of the local oceanographic settings. It is not driven simply by latitudinally dependent light availability.
2) The seasonality of the flux may be transferred to sediments, but this signal can be altered due to the complexity of sedimentation processes. Export in seasons of low alkenone production in surface waters appear to be less attenuated with depth than in seasons of high alkenone production.
3) The $U^{K'}_{37}$ export signals in some locations may be seasonally biased, but the resemblance between the global trends in $U^{K'}_{37}$ in surface sediments and the flux weighted $\bar{U}^{K'}_{37}$ from sediment traps demonstrate that sedimentary SST estimates from $U^{K'}_{37}$ correspond most significantly with annual averages. Without the availability of independent biogeochemical measures complementary to $U^{K'}_{37}$, the oceanographic interpretation of $U^{K'}_{37}$ values recorded in sediments as a measure of annual mean SST cannot be refined.

From a paleoceanographic perspective, sediment trap times series studies like those reviewed here are necessary to achieve the ultimate goal of explaining which processes lead to the accumulation of alkenones in surface sediments. Further studies would provide more evidence to advance a robust, mechanistic understanding of non-random, regional variation in the core-top calibration of $U^{K'}_{37}$ vs annual mean SST, and potentially refine the quality of paleoceanographic interpretations drawn from stratigraphic alkenone records.

Acknowledgements

Support for this work was provided with funding to A.R.M. by the European Commission (Marie Curie-IOF, 235626; and P4F project XXXX) and to F.G.P. by the U.S. National Science Foundation (OCE-1204204).

Figure 1. A) Relative annually averaged fluxes (in logarithmic scale) among the sediment traps from Table 1. Sites with highest fluxes are in red, while those with lowest are in blue. B) Values of residual for temperature estimates at each sediment trap time series location. Residual temperature is defined as the difference between water temperature estimated from alkenone flux weighted values of the alkenone unsaturation index ($\bar{U}^{K'}_{37}$), derived using the global core top calibration equation $U^{K'}_{37} = 0.033\ T + 0.044$ (Müller et al., 1998a), and mean annual sea-surface temperature obtained from quarter degree resolution 2001 World Ocean Atlas (Conkright et al., 2002).

Figure 2. Map of polar plots summarizing the annual alkenone fluxes in the water column measured using sediment traps from all studies listed in Table 1. Each wedge corresponds to a sampling time interval, whose angle is then used to represent the time of the year (e.g. 0° corresponds to 1st January). The radius or length of each wedge correspond to the values of the alkenone flux (μg m^{-2} d^{-1}) in logarithmic scale normalized to the maximum and minimum value (rounded to nearest and lower decimal value, i.e. 10, 1, 0.1 etc.) in the particular study. The colors are used to identify seasons: red for July-September, brown for October-December, blue for January-March and green for April-June.

Figure 3. A) Scatter plot illustrating the relationship between annual alkenone flux weighted values of the alkenone unsaturation index ($\bar{U}^{K'}_{37}$) derived from sediment trap time series measurements and mean annual sea-surface temperature (solid circles) obtained from quarter degree resolved 2001 World Ocean Atlas (Conkright et al., 2002). The $U^{K'}_{37}$ – SST calibration relationship for both global surface sediments (solid black line, ±2°C – dashed black lines) (Müller et al., 1998a) and for suspended particulate material collected from surface waters throughout the global ocean (solid grey line) (Conte et al., 2006) are shown for reference purposes. Sites where the data appear to fall significantly outside the 'expected' linear trend are identified and labelled as 'cold outliers'. The 'error bars' depict the seasonal range of SST reported in the World Ocean Atlas at each of these sites. B) Scatter plot illustrating relationship between annual K37s flux weighted values of the alkenone unsaturation index ($\bar{U}^{K'}_{37}$), and $U^{K'}_{37}$ values measured in surface sediments from the underlying sediment trap sites. A 1:1 line is shown for reference purposes.

Figure 4. Maps of SST (A) and nitrate (B) based on data from the one degree resolution World Ocean Atlas 2001 (Conkright et al., 2002). Black circles denote the locations of sediment trap sampling sites where residual $\bar{U}^{K'}_{37}$-based estimates of mean annual SST (as in

Fig. 1B) are larger than -2.5°C. These sites correspond to the specifically labeled points in Fig. 3A.

Table 1. Summary of alkenone (K37s) flux and unsaturation index (flux weighted $\bar{U}^{K'}_{37}$ and non-weighted $U^{K'}_{37}$ averages) data compilation for available sediment trap time series in the ocean either published or unpublished. The timing of maximum production corresponds to those periods identified by the authors in the original study. The seasons (boreal or austral) have been defined for the intervals December-February (winter or summer), March-May (spring or autumn), June-August (summer or winter), and September-November (autumn or spring). Where available, flux data are provided for the different depths of sediment trap collection in each study.*(Number of days of each sampling period at depth 1, depth 2, etc).

Table 1

Latitude Longitude	Area	Sampling Period [days]*	Trap Depth (m)	Average Flux [min-max] (µg m^{-2} d^{-1})	Timing of Maximum Flux	Flux-weighted $\bar{U}^{K'}_{37}$ [$U^{K'}_{37}$]	SST mean annual [winter – summer] (^{o}C)	Reference
75°11.8'N 012°29'E	Barents Sea continental margin	3/1991 - 7/1991 [129, 129]	1840 1950	0.27 [0.01-2.77] 0.18 [0.01-0.63]	June-July	0.210 [0.265] 0.787 [0.724]	4.7 [3.8, 6.6]	(Thomsen, 1993; Thomsen et al., 1998)
69°41'N 0°28'E	Norwegian Sea	8/1991 - 7/1992 [76, 76, 76]	500 1000 3000	0.07 [0.01-0.14] 0.02 [0.02-0.04] 0.07 [0.01-0.13]	October / November; May	No reliable $U^{K'}_{37}$ data	6.4 [4.6, 9.0]	(Thomsen, 1993; Thomsen et al., 1998)
70°00'N 0°0.6'W	Norwegian Sea	8/1992- 7/1993 [398, 298, 367]	500 1000 3000	0.17 [0.01-0.59] 0.26 [0.01-1.4] 0.21 [0.06-0.88]	June-September	0.292 [0.307] 0.295 [0.299] 0.311 [0.324]	5.9 [4.0, 8.5]	(Flügge, 1997)
70°00'N 0°4'W	Norwegian Sea	7/1994- 7/1995 [367, 367]	1000 2500	0.11 [0.01-1.50] 0.31 [0.01-1.31]	June-September	0.258 [0.259] 0.256 [0.267]	4.9 [3.0, 7.6]	(Flügge, 1997)
53°3'N 176°59'W	Aleutian Basin	8/1994- 7/1995 [355]	3198	0.19 [0.01-0.86]	November	0.277 [0.316]	5.5 [3.3, 8.6]	Prahl & Takahashi, unpublished
49°01'N 174°W	Subarctic Pacific	8/1994- 7/1995 [355]	4774	0.37 [0.03-2.4]	November	0.337 [0.385]	6.6 [3.9, 10]	Prahl & Takahashi, unpublished

53°00'N 145°30'E	Sea of Okhotsk	8/1999 - 6/2000 [639, 639]	270 1540	1.1 [0.03-5.8] 0.4 [0.02-1.5]	Autumn	0.265 [0.275] 0.286 [0.293]	3.5 [-1.7, 11.1]	(Seki et al., 2007)
49°31'N 146°30'E	Sea of Okhotsk	9/1999-6/2000 [594, 594]	270 685	0.81 [0.04-3.2] 0.29 [0.02-0.65]	Autumn	0.246 [0.229] 0.255 [0.264]	4.0 [-1.2, 10.8]	(Seki et al., 2007)
48°N 21°W	NE Atlantic	4/1989 - 3/1990 [373]	3700	0.75 [0..08-4.5]	April-August	0.408 [0.425]	14.3 [12.2, 17.1]	(Rosell-Melé et al., 2000)
40°00'N 165°01'E	Subarctic NW Pacific	12/1997- 12/1998 [366]	2986	6.6 [0.5-49]	October	0.614 [0.539]	13.9 [10.1, 18.7]	(Harada et al., 2006)
43°58'N 155°03'E	Subarctic NW Pacific	12/1997 - 5/1999 [503]	2957	4.2 [0.5-19]	July-October	0.406 [0.450]	8.0 [3.2, 13.9]	(Harada et al., 2006)
50°01'N 165°01'E	Subarctic NW Pacific	12/1997 - 5/1999 [389]	3260	1.2 [0.16-6.6]	November	0.284 [0.314]	5.3 [2.2, 9.8]	(Harada et al., 2006)
43°25'N 7°52'E	Ligurian Sea, Mediterranean	2/1989 - 3/1990 5/1993 - 11/1994 [618]	200	1.3 [0-16]	Autumn (major), May (minor)	0.489 [0.472]	17.4 [13.2,22.5]	(Sicre et al., 1999; Ternois et al., 1996; Ternois et al., 1997)
42°28'N 138°30'E	Sea of Japan (East Sea)	10/2000 – 8/2001 [338,338]	1057 3043	0.01 [0-0.03] 0.001[0-0.003]	Summer-Autumn	0.481 [0.500] 0.442 [0.478]	11.6 [5.0, 20.1]	(Lee et al., 2011)

38°01’N 135°01’E	Sea of Japan (East Sea)	10/2000 – 8/2001 [312, 312]	1057 2100	0.02 [0.01-0.06] 0.01 [0-0.04]	Summer-Autumn	0.605 [0.561] 0.563 [0.598]	16.2 [10, 23.6]	(Lee et al., 2011)
42°40’N 69°45’W	Wilkinson Basin, Gulf of Maine	3/1995 - 12/1995 [264]	225	14.3 (0.4-115]	September-November	0.376 [0.348]	9.8 [4.1, 16.7]	(Prahl et al., 2001)
41°34’N 141°52’E	NW Pacific, off Japan	6/2002 – 6/2003 [315]	350	34.6 [0.3-245]	June-July	0.454 [0.499]	11.3 [4.4, 18.8]	(Kawahata et al., 2009)
39°00’N 147°00’E	NW Pacific	11/1997 - 8/1999 [571, 612, 556]	1366 3056 4786	6.0 [0.75-30] 3.1 [0.92-14] 1.7 [0.37-15]	Two seasonal cycles: increased spring to fall, then opposite	0.546 [0.581] 0.566 [0.602] 0.550 [0.608]	15.3 [10.2, 21.7]	(Yamamoto et al., 2007)
34°9.6’N 120°15.6’ W	Santa Barbara Basin	8/1993 – 4/2004 [1109]	490	15.4 [0.21-132]	no consistent seasonality	0.518 [0.526]	14.8 [13.4, 16.5]	(Hardee, unpublished)
34°10’N 142°E	northwestern North Pacific off Japan	3/1991-3/1992 [364, 364, 364, 196]	1674 4180 5687 8688	4.0 [0.55-17] 3.3 [0.87-6.6] 2.2 [0.38-5.8] 2.5 [1.3-3.9]	Late Spring-Summer	0.756 [0.749] 0.736 [0.734] 0.740 [0.734] 0.716 [0.714]	21.9 [18.1, 26.5]	(Sawada et al., 1998)
42°05’N 125°45’W	NE Pacific	9/1987 – 8/1988 [360]	1000	4.2 [1.9-7.6]	May-June	0.381 [0.399]	12.5 [10.5, 14.6]	(Prahl et al., 1993); unpublished

42°10'N 127°35'W	NE Pacific	9/1987 – 4/1989 [360, 364, 360]	1000 1500 1750	2.9 [0.58-9.1] 1.9 [0.49-4.4] 1.7 [0.55-5.8]	May-June	0.375 [0.411] 0.368 [0.370] 0.345 [0.367]	13.3 [10.7, 16.5]	(Prahl et al., 1993); unpublished
42°30'N 132°W	NE Pacific	9/1987 – 4/1989 [360, 364]	1000 1500	3.7 [0.27-19] 2.2 [0.16-9.6]	May-June	0.334 [0.380] 0.307 [0.350]	14.3 [11.7, 17.5]	(Prahl et al., 1993); unpublished
33°N 22°W	NE Atlantic	9/1989-6/1993 [1295]	2000	0.91 [0.01-8.4]	February-March	n.a.	20.7 [18.2, 23.5]	(Waniek et al., 2005)
27°53'N 111°40'W	Gulf of California	1/1996 – 9/1997 [293]	500	7.0 [2.0-14]	June-October	0.873 [0.828]	23.4 [16.7, 30.2]	(Goñi et al., 2001)
22°45'N 158°W	North Pacific Subtropical Gyre	6/1992-5/1993 and 12/2000-11/2001 [681]	2800	0.29 [0.07-1.6]	winter and summer	0.857 [0.873]	24.7 [23.4, 26]	(Prahl et al., 2005)
20°45.3'N 19°44.5'W	Cape Blanc, NW Africa	3/1988 – 3/1989 [351]	2195	3.1 [0.70-7.9]	no consistent seasonality	0.807 [0.808]	21.4 [19.6, 23.1]	(Müller and Fischer, 2001)
21°08.7'N 20°41.2'W	Cape Blanc, NW Africa	3/1989-11/1991 [577, 886]	730 3562	20.4 [0.30-233] 6.4 [0.40-84]	no consistent seasonality	0.764 [0.793] 0.795 [0.806]	22 [20.2, 23.5]	(Müller and Fischer, 2001)
15°59'N 61°30'E	Central Arabian Sea	11/1994-11/1995 [272, 374]	821 2229	9.0 [0.57-49] 6.2 [0.87-41]	NE and SW monsoons (beginning and end)	0.958 [0.950] 0.951 [0.950]	27 [25.6, 26.3]	(Prahl et al., 2000)

10°30'N 64°40'W	Cariaco Basin	11/1996 - 10/1999 [580]	275 455 930	16.3 [0.61-63] 15.2 [0.58-70] 12.7 [2.5-28]	no consistent seasonality	0.901 [0.903] 0.871 [0.893] 0.883 [0.898]	26.1 [24.8, 26.5]	(Goni et al., 2004; Goñi et al., 2003)
0°N 175°E	West equatorial Pacific	9/1992 - 8/1993 [336, 338]	1770 4220	0.27 [0.05-0.84] 0.12 [0.05-0.25]	November, February-March, June	0.967 [0.982] 0.982 [0.983]	28.7 [28.2, 29.1]	(Harada et al., 2001)
42°42'S 178°38'E	western South Pacific, east of New Zealand	9/1996–4/1997 [208]	300	5.2 [0.07-23]	October, January	0.421 [0.453]	15.7 [13.4, 18.3]	(Sikes et al., 2005)
44°37'S 178°37'E	western South Pacific, east of New Zealand	6/1996-4/1997 [176]	300	6.7 [0.09-22]	August-December	0.268 [0.359]	13.3 [11.3, 15.8]	(Sikes et al., 2005)
50°40'S 68°25'E	Indian Ocean sector of the Southern Ocean	4/1993 - 1/1994 [170]	200	1.6 [0.10-9.3]	January (major) April/May (minor)	0.039 [0.037]	3.6 [2.6, 5]	(Ternois et al., 1998)

References

Bard, E., 2001. Comparison of alkenone estimates with other paleotemperature proxies. Geochem Geophy Geosy 2, U1-U12. DOI: 10.1029/2000GC000050

Behrenfeld, M.J., O'Malley, R.T., Siegel, D.A., McClain, C.R., Sarmiento, J.L., Feldman, G.C., Milligan, A.J., Falkowski, P.G., Letelier, R.M., Boss, E.S., 2006. Climate-driven trends in contemporary ocean productivity. Nature 444, 752-755. Doi 10.1038/Nature05317

Bendle, J., Rosell-Melé, A., 2004. Distributions of $U^{K'}37$ and $U^{K'}_{37}$ in the surface waters and sediments of the Nordic Seas: Implications for paleoceanography. Geochem Geophy Geosy 5. DOI: 10.1029/2004GC000741

Bentaleb, I., Fontugne, M., Beaufort, L., 2002. Long-chain alkenones and $U^{K'}_{37}$ variability along a south-north transect in the Western Pacific Ocean. Global Planet. Change 34, 173-183.

Benthien, A., Muller, P.J., 2000. Anomalously low alkenone temperatures caused by lateral particle and sediment transport in the Malvinas Current region, western Argentine Basin. Deep-Sea Res Pt I 47, 2369-2393.

Brassell, S.C., 1993. Applications of biomarkers for delineating marine palaeoclimatic fluctuations during the Pleistocene, In: Engel, M.H., Macko, S.A. (Eds.), Organic Geochemistry Principles and Applications. Plenum Press, New York, pp. 699-738.

Brassell, S.C., Eglinton, G., Marlowe, I.T., Pflaumann, U., Sarnthein, M., 1986. Molecular stratigraphy: a new tool for climatic assessment. Nature 320, 129-133.

Conkright, M.E., Locarnini, R.A., Garcia, H.E., O'Brien, T.D., Boyer, T.P., Stephen, C., Antonov, J.I., 2002. World Ocean Atlas 2001: Objective Analyses, Data Statistics, and Figures, CD-ROM Documentation. National Oceanographic Data Center, Silver Spring, MD.

Conte, M.H., Dickey, T.D., Weber, J.C., Johnson, R.J., Knap, A.H., 2003. Transient physical forcing of pulsed export of bioreactive material to the deep Sargasso Sea. Deep-Sea Research Part I: Oceanographic Research Papers 50, 1157-1187. DOI: 10.1029/2000JC000589

Conte, M.H., Eglinton, G., 1993. Alkenone and alkenoate distributions within the euphotic zone of the eastern north Atlantic: correlation with production temperature. Deep-Sea Research I 40, 1935-1961.

Conte, M.H., Eglinton, G., Madureira, L.A.S., 1992. Long-chain alkenones and alkyl alkenoates as palaeotemperature indicators: their production, flux and early sedimentary diagenesis in the Eastern North Atlantic. Organic Geochemistry 19, 287-298.

Conte, M.H., Sicre, M.A., Ruhlemann, C., Weber, J.C., Schulte, S., Schulz-Bull, D., Blanz, T., 2006. Global temperature calibration of the alkenone unsaturation index (UK37') in surface waters and comparison with surface sediments. Geochem Geophy Geosy 7, doi:10.1029/2005GC001054.

Conte, M.H., Thompson, A., Lesley, D., Harris, R.P., 1998a. Genetic and physiological influences on the alkenone/alkenoate versus growth temperature relationship in Emiliania huxleyi and Geophyrocapsa oceanica. Geochim. Cosmochim. Acta 62, 51-68.

Conte, M.H., Weber, J.C., Ralph, N., 1998b. Episodic particle flux in the deep Sargasso Sea: an organic geochemical assessment. Deep-Sea Research I 45, 1819-1841.

Chapman, M.R., Shackleton, N.J., Zhao, M., Eglinton, G., 1996. Faunal and alkenone reconstructions of subtropical North Atlantic surface hydrography and palaeotemperature over the last 28kyr. Paleoceanography 11, 343-358.

de Leeuw, J.W., van de Meer, F.W., Rijpstra, W.I.C., Schenck, P.A., 1980. On the occurrence and structural identification of long chain unsaturated ketones and hydrocarbons in sediments., In: Douglas, A.G., Maxwell, J.R. (Eds.), Advances in Organic Geochemistry 1979. Pergamon, Oxford, pp. 211-217.

de Vernal, A., Rosell-Mele, A., Kucera, M., Hillaire-Marcel, C., Eynaud, F., Weinelt, M., Dokken, T., Kageyama, M., 2006. Comparing proxies for the reconstruction of LGM sea-surface conditions in the northern North Atlantic. Quat. Sci. Rev. 25, 2820-2834.

Doose, H., Prahl, F.G., Lyle, M.W., 1997. Biomarker temperature estimates for modern and last glacial surface waters of the California Current system between 33 degrees and 42 degrees N. Paleoceanography 12, 615-622.

Fischer, H., Schmitt, J., Lüthi, D., Stocker, T.F., Tschumi, T., Parekh, P., Joos, F., Köhler, P., Völker, C., Gersonde, R., Barbante, C., Le Floch, M., Raynaud, D., Wolff, E., 2010. The role of Southern Ocean processes in orbital and millennial CO2 variations – A synthesis. Quat. Sci. Rev. 29, 193-205. 10.1016/j.quascirev.2009.06.007

Flügge, A., 1997. Jahreszeitliche Variabilität von ungesüttigten C_{37} methylketonen in sinkstofffallenmaterial der Norwegischen See und deren Abbildung in Oberflächensedimenten. PhD Thesis. Universität zu Kiel.

François, R., Honjo, S., Krishfield, R., Manganini, S., 2002. Factors controlling the flux of organic carbon to the bathypelagic zone of the ocean. Global Biogeochem. Cycles 16, 1087. 10.1029/2001gb001722

Giraud, X., 2006. Modelling an alkenone-like proxy record in the NW African upwelling. Biogeosciences 3, 251-269.

Goni, M.A., Woodworth, M.P., Aceves, H.L., Thunell, R.C., Tappa, E., Black, D., Muller-Karger, F., Astor, Y., Varela, R., 2004. Generation, transport, and preservation of the alkenone-based UK37' sea surface temperature index in the water column and sediments of the Cariaco Basin (Venezuela). Global Biogeochemical Cycles 18. doi:10.1029/2003GB002132

Goñi, M.A., Aceves, H.L., Thunell, R.C., Tappa, E., Black, D., Astor, Y., Varela, R., Muller-Karger, F., 2003. Biogenic fluxes in the Cariaco Basin: a combined study of sinking particulates and underlying sediments. Deep Sea Research Part I: Oceanographic Research Papers 50, 781-807. Doi: 10.1016/s0967-0637(03)00060-8

Goñi, M.A., Hartz, D.M., Thunell, R.C., Tappa, E., 2001. Oceanographic considerations for the application of the alkenone-based paleotemperature U-37(K ') index in the Gulf of California. Geochim. Cosmochim. Acta 65, 545-557.

Harada, N., Handa, N., Harada, K., Matsuoka, H., 2001. Alkenones and particulate fluxes in sediment traps from the central equatorial Pacific. Deep-Sea Res Pt I 48, 891-907.

Harada, N., Sato, M., Shiraishi, A., Honda, M.C., 2006. Characteristics of alkenone distributions in suspended and sinking particles in the northwestern North Pacific. Geochim. Cosmochim. Acta 70, 2045-2062.

Haug, G.H., Ganopolski, A., Sigman, D.M., Rosell-Mele, A., Swann, G.E.A., Tiedemann, R., Jaccard, S.L., Bollmann, J., Maslin, M.A., Leng, M.J., Eglinton, G., 2005. North Pacific seasonality and the glaciation of North America 2.7 million years ago. Nature 433, 821-825.

Herbert, T.D., Schuffert, J.D., Thomas, D., Lange, C., Weinheimer, A., Peleo-Alampay, A., Herguera, J.-C., 1998. Depth and seasonality of alkenone production along the California margin inferred from a core top transect. Paleoceanography 13, 263-271.

Honjo, S., Manganini, S.J., Krishfield, R.A., Francois, R., 2008. Particulate organic carbon fluxes to the ocean interior and factors controlling the biological pump: A synthesis of global sediment trap programs since 1983. Progress In Oceanography 76, 217-285. 10.1016/j.pocean.2007.11.003

Kawahata, H., Minoshima, K., Ishizaki, Y., Yamaoka, K., Gupta, L.P., Nagao, M., Kuroyanagi, A., 2009. Comparison of settling particles and sediments at IMAGES coring site in the northwestern North Pacific -- Effect of resuspended particles on paleorecords. Sedimentary Geology 222, 254-262. DOI: 10.1016/j.sedgeo.2009.09.012

Kienast, M., MacIntyre, G., Dubois, N., Higginson, S., Normandeau, C., Chazen, C., Herbert, T.D., 2012. Alkenone unsaturation in surface sediments from the eastern equatorial Pacific: Implications for SST reconstructions. Paleoceanography 27. Artn Pa1210 Doi 10.1029/2011pa002254

Leduc, G., Schneider, R., Kim, J.H., Lohmann, G., 2010. Holocene and Eemian sea surface temperature trends as revealed by alkenone and Mg/Ca paleothermometry. Quat. Sci. Rev. 29, 989-1004. DOI 10.1016/j.quascirev.2010.01.004

Lee, K.E., Khim, B.K., Otosaka, S., Noriki, S., 2011. Sediment trap record of alkenones from the East Sea (Japan Sea). Organic Geochemistry 42, 255-261. DOI 10.1016/j.orggeochem.2010.12.008

Lutz, M.J., Caldeira, K., Dunbar, R.B., Behrenfeld, M.J., 2007. Seasonal rhythms of net primary production and particulate organic carbon flux to depth describe the efficiency of biological pump in the global ocean. J. Geophys. Res. 112, C10011. 10.1029/2006jc003706

Martínez-Garcia, A., Rosell-Melé, A., Geibert, W., Gersonde, R., Masque, P., Gaspari, V., Barbante, C., 2009. Links between iron supply, marine productivity, sea surface temperature, and CO_2 over the last 1.1 Ma. Paleoceanography 24, PA1207. 10.1029/2008pa001657

Müller, P.J., Fischer, G., 2001. A 4-year sediment trap record of alkenones from the filamentous upwelling region off Cape Blanc, NW Africa and a comparison with distributions in underlying sediments. Deep-Sea Res Pt I 48, 1877-1903.

Müller, P.J., Kirst, G., Ruhland, G., von Storch, I., Rosell-Melé, A., 1998a. Calibration of the alkenone paleotemperature index $U_{37}^{K'}$ based on core-tops from the eastern South Atlantic and the global ocean (60 °N-60 °S). Geochim. Cosmochim. Acta 62, 1757-1772. 10.1016/S0016-7037(98)00097-0

Müller, P.J., Kirst, G., Ruhland, G., von Storch, I., Rosell-Melé, A., 1998b. Calibration of the alkenone paleotemperature index U-37(K ') based on core-tops from the eastern South Atlantic and the global ocean (60 degrees N-60 degrees S). Geochim. Cosmochim. Acta 62, 1757-1772.

Ohkouchi, N., Kawamura, K., Kawahata, H., Okada, H., 1999. Depth ranges of alkenone production in the Central Pacific Ocean. Global Biogeochemical Cycles 13, 695-704.

Pelejero, C., Calvo, E., 2003. The upper end of the $U^{K'}_{37}$ temperature calibration revisited. Geochem Geophy Geosy 4, art. no.-1014.

Pichon, J.J., Sikes, E.L., Hiramatsu, C., Robertson, L., 1998. Comparison of $U^{K'}_{37}$ and diatom assemblage sea surface temperature estimates with atlas derived data in holocene sediments from the southern west Indian Ocean. Journal of Marine Systems 17, 541-554.

Prahl, F.G., Collier, R.B., Dymond, J., Lyle, M., Sparrow, M.A., 1993. A biomarker perspective on prymnesiophyte in the northeast Pacific Ocean. Deep-Sea Research I 40, 2061-2076.

Prahl, F.G., Dymond, J., Sparrow, M., 2000. Annual biomarker record for export production in the central Arabian Sea. deep-Sea Research II 47, 1581-1604.

Prahl, F.G., Mix, A.C., Sparrow, M.A., 2006. Alkenone paleothermometry: Biological lessons from marine sediment records off western South America. Geochim. Cosmochim. Acta 70, 101-117.

Prahl, F.G., Muehlhausen, L.A., Zahnle, D.I., 1988. Further evaluation of long-chain alkenones as indicators of paleoceanographic conditions. Geochim. Cosmochim. Acta 52, 2303-2310.

Prahl, F.G., Pilskaln, C.H., Sparrow, M.A., 2001. Seasonal record for alkenones in sedimentary particles from the Gulf of Maine. Deep-Sea Res Pt I 48, 515-528.

Prahl, F.G., Popp, B.N., Karl, D.M., Sparrow, M.A., 2005. Ecology and biogeochemistry of alkenone production at Station ALOHA. Deep-Sea Res Pt I 52, 699-719.

Prahl, F.G., Rontani, J.F., Zabeti, N., Walinsky, S.E., Sparrow, M.A., 2010. Systematic pattern in $U^{K37'}$ - Temperature residuals for surface sediments from high latitude and other oceanographic settings. Geochim. Cosmochim. Acta 74, 131-143.

Prahl, F.G., Wakeham, S.G., 1987. Calibration of unsaturation patterns in long-chain ketone compositions for palaeotemperature assessment. Nature 320, 367-369.

Rosell-Melé, A., Comes, P., Müller, P.J., Ziveri, P., 2000. Alkenone fluxes and anomalous U37K' values during 1989-1990 in the Northeast Atlantic (48°N 21°W). Mar. Chem. 71, 251-264.

Rosell-Mele, A., Eglinton, G., Pflaumann, U., Sarnthein, M., 1995. Atlantic core-top calibration of the Uk37 index as a sea-surface palaeotemperature indicator. Geochim. Cosmochim. Acta 59, 3099-3107.

Rühlemann, C., Butzin, M., 2006. Alkenone temperature anomalies in the Brazil-Malvinas Confluence area caused by lateral advection of suspended particulate material. Geochem. Geophys. Geosyst. 7. DOI: 10.1029/2006GC001251

Sawada, K., Handa, N., Nakatsuka, T., 1998. Production and transport of long-chain alkenones and alkyl alkenoates in a sea water column in the northwestern Pacific off central Japan. Mar. Chem. 59, 219-234. Doi: 10.1016/s0304-4203(97)00074-1

Schneider, B., Leduc, G., Park, W., 2010. Disentangling seasonal signals in Holocene climate trends by satellite-model-proxy integration. Paleoceanography 25, PA4217. 10.1029/2009pa001893

Seki, O., Nakatsuka, T., Kawamura, K., Saitoh, S.-I., Wakatsuchi, M., 2007. Time-series sediment trap record of alkenones from the western Sea of Okhotsk. Mar. Chem. 104, 253-265. DOI: 10.1016/j.marchem.2006.12.002

Sicre, M.A., Ternois, Y., Miquel, J.C., Marty, J.C., 1999. Alkenones in the Northwestern Mediterranean sea: interannual variability and vertical transfer. Geophys. Res. Lett. 26, 1735-1738.

Sikes, E.L., Farrington, J.W., Keigwin, L.D., 1991. Use of the alkenone unsaturation ratio $U^{K'}_{37}$ to determine past sea surface temperatures: core-top SST calibrations and methodology considerations. Earth Planet. Sci. Lett. 104, 36-47.

Sikes, E.L., Howard, W.R., Neil, H.L., Volkman, J.K., 2002. Glacial-interglacial sea surface temperature changes across the subtropical front east of New Zealand based on alkenone unsaturation ratios and foraminiferal assemblages. Paleoceanography 17. DOI: 10.1029/2001PA000640

Sikes, E.L., O'Leary, T., Nodder, S.D., Volkman, J.K., 2005. Alkenone temperature records and biomarker flux at the subtropical front on the chatham rise, SW Pacific Ocean. Deep-Sea Res Pt I 52, 721-748.

Sonzogni, C., Bard, E., Rostek, F., Lafont, A., Rosell-Mele, A., Eglinton, G., 1997. Core-top calibration of the alkenone index versus sea surface temperature in the Indian Ocean. Deep-Sea Research 44, 1445-1460.

Ternois, Y., Sicre, M.-A., Boireau, A., Marty, J.-C., Miquel, J.-C., 1996. Production pattern of alkenones in the Mediterranean Sea. Geophys. Res. Lett. 23, 3171-3174.

Ternois, Y., Sicre, M.A., Boireau, A., Beaufort, L., Miquel, J.C., Jeandel, C., 1998. Hydrocarbons, sterols and alkenones in sinking particles in the Indian Ocean sector of the Southern Ocean. Organic Geochemistry 28, 489-501.

Ternois, Y., Sicre, M.A., Boireau, A., Conte, M.H., Eglinton, G., 1997. Evaluation of long-chain alkenones as paleo-temperature indicators in the Mediterranean Sea. Deep-Sea Research I 44, 271-286.

Thomsen, C., 1993. Verfolgung pelagischer Prozesse mit Hilfe ciochemischen Komponenten am Beispiel der Alkenone (C37:2, C37:2). PhD Thesis., Matematisch-Naturwissenschaftlichen Fakultät. Christian-albrechts Universität, Kiel, p. 94.

Thomsen, C., Schulz-Bull, D.E., Petrick, G., Duinker, J.C., 1998. Seasonal variability of the long-chain alkenone flux and the effect on the $U^{K'}_{37}$ index in the Norwegian Sea. Organic Geochemistry 28, 311-323.

Volkman, J.K., Eglinton, G., Corner, E.D.S., Forsberg, T.E.V., 1980. Long-chain alkenes and alkenones in the marine coccolithophorid Emiliania huxleyi. Phytochemistry 19, 2619-2622.

Waelbroeck, C., Paul, A., Kucera, M., Rosell-Mele, A., Weinelt, M., Schneider, R., Mix, A.C., Abelmann, A., Armand, L., Bard, E., Barker, S., Barrows, T.T., Benway, H., Cacho, I., Chen, M.T., Cortijo, E., Crosta, X., de Vernal, A., Dokken, T., Duprat, J., Elderfield, H., Eynaud, F., Gersonde, R., Hayes, A., Henry, M., Hillaire-Marcel, C., Huang, C.C., Jansen, E., Juggins, S., Kallel, N., Kiefer, T., Kienast, M., Labeyrie, L., Leclaire, H., Londeix, L., Mangin, S., Matthiessen, J., Marret, F., Meland, M., Morey, A.E., Mulitza, S., Pflaumann, U., Pisias, N.G., Radi, T., Rochon, A., Rohling, E.J., Sbaffi, L., Schafer-Neth, C., Solignac, S., Spero, H., Tachikawa, K., Turon, J.L., 2009. Constraints on the magnitude and patterns of ocean cooling at the Last Glacial Maximum. Nature Geoscience 2, 127-132.

Waniek, J.J., Schulz-Bull, D.E., Blanz, T., Prien, R.D., Oschlies, A., Müller, T.J., 2005. Interannual variability of deep water particle flux in relation to production and lateral sources in the northeast Atlantic. Deep Sea Research Part I: Oceanographic Research Papers 52, 33-50. DOI: 10.1016/j.dsr.2004.08.008

Wolhowe, M.D., Prahl, F.G., Probert, I., Maldonado, M., 2009. Growth phase dependent hydrogen isotopic fractionation in alkenone-producing haptophytes,. Biogeosciences 6, 1681-1694.

Yamamoto, M., Shimamoto, A., Fukuhara, T., Naraoka, H., Tanaka, Y., Nishimura, A., 2007. Seasonal and depth variations in molecular and isotopic alkenone composition of sinking particles from the western North Pacific. Deep-Sea Res Pt I 54, 1571-1592.

*Figure

Figure 1A

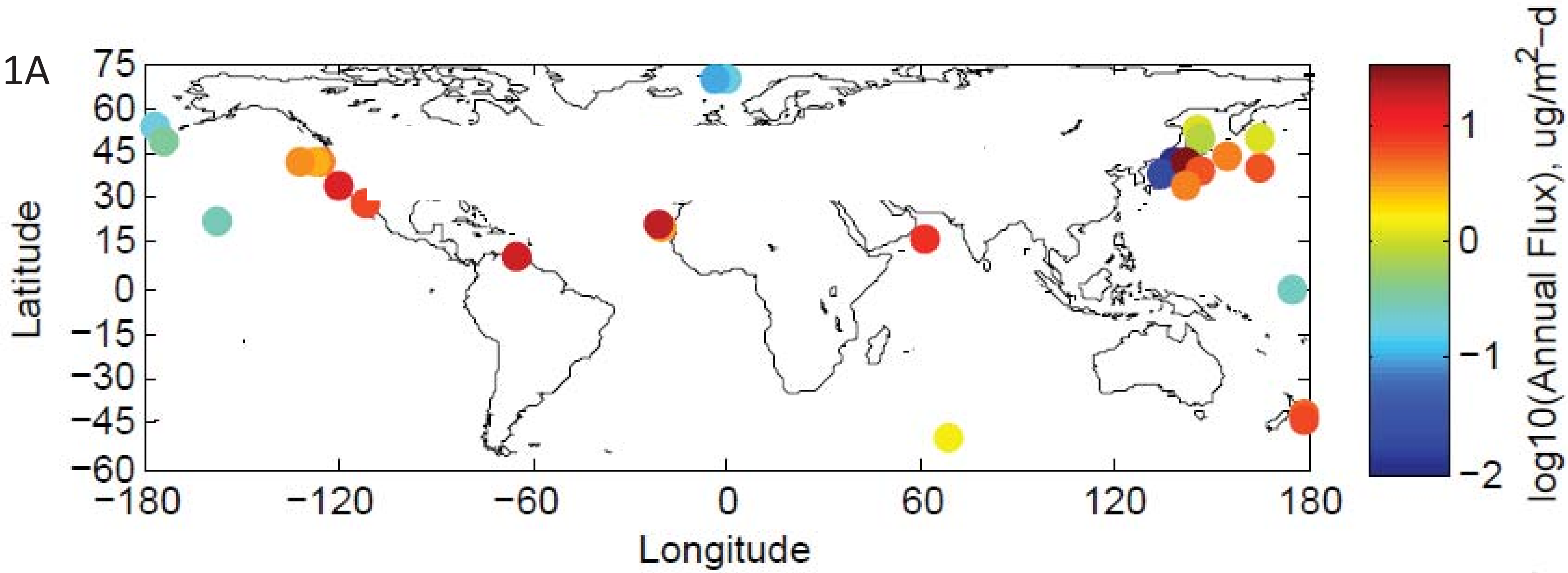

Figure 1B

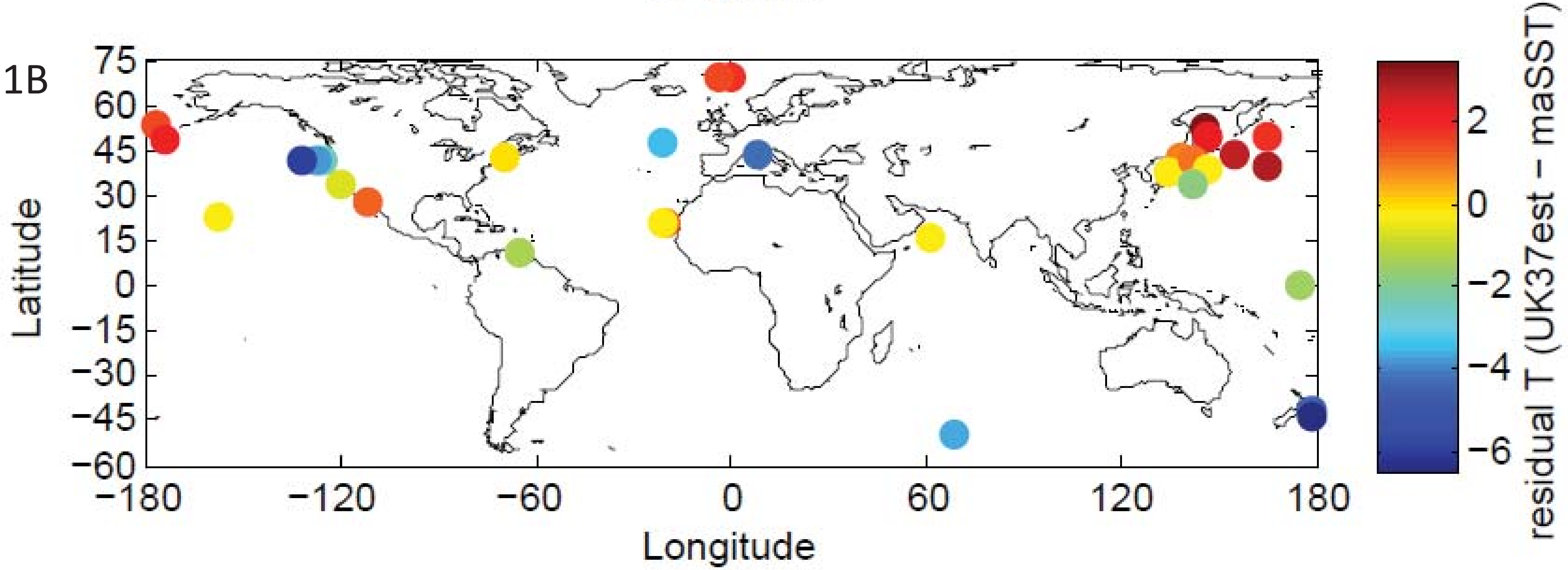

Figure 2

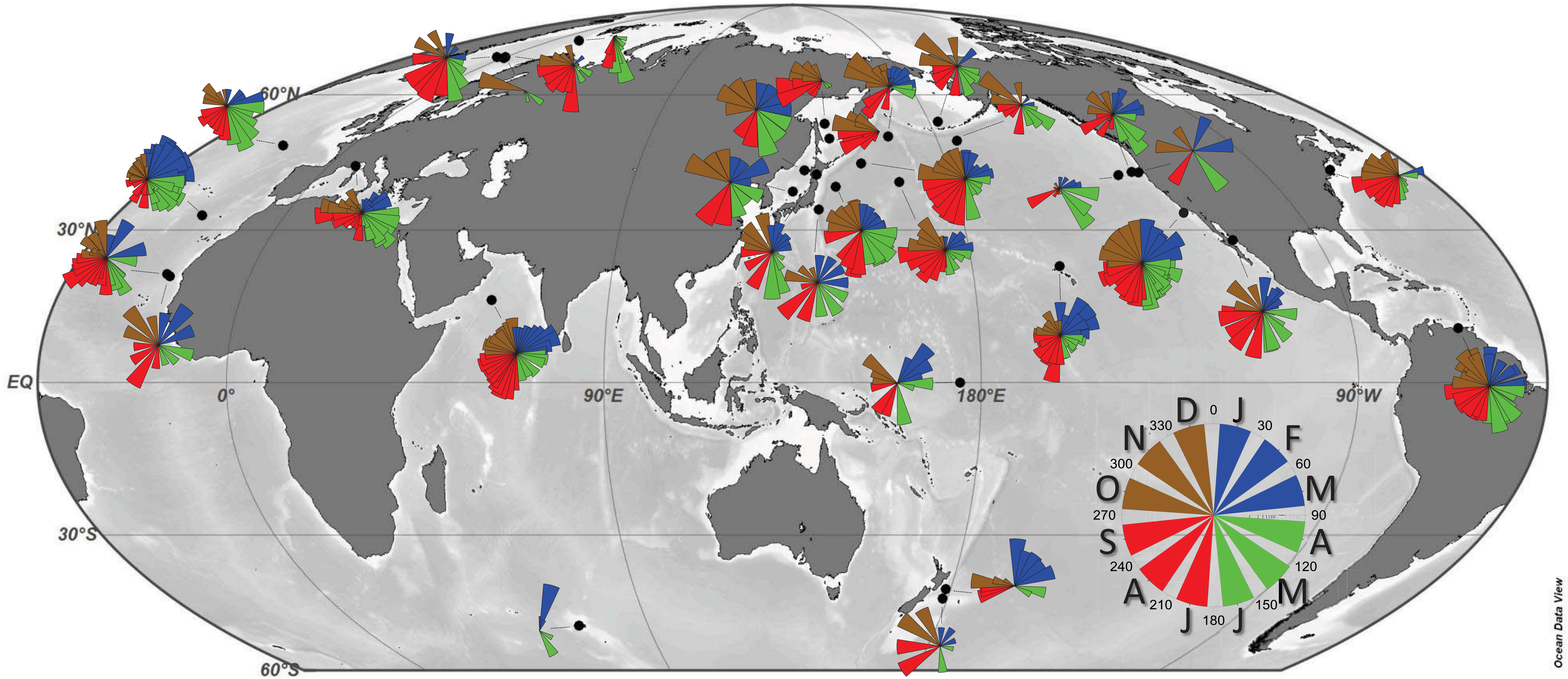
60°N
30°N
EQ
30°S
60°S
0°
90°E
180°E
90°W
D
J
F
M
A
M
J
J
A
S
O
N
0
30
60
90
120
150
180
210
240
270
300
330
Ocean Data View

Figure 3A

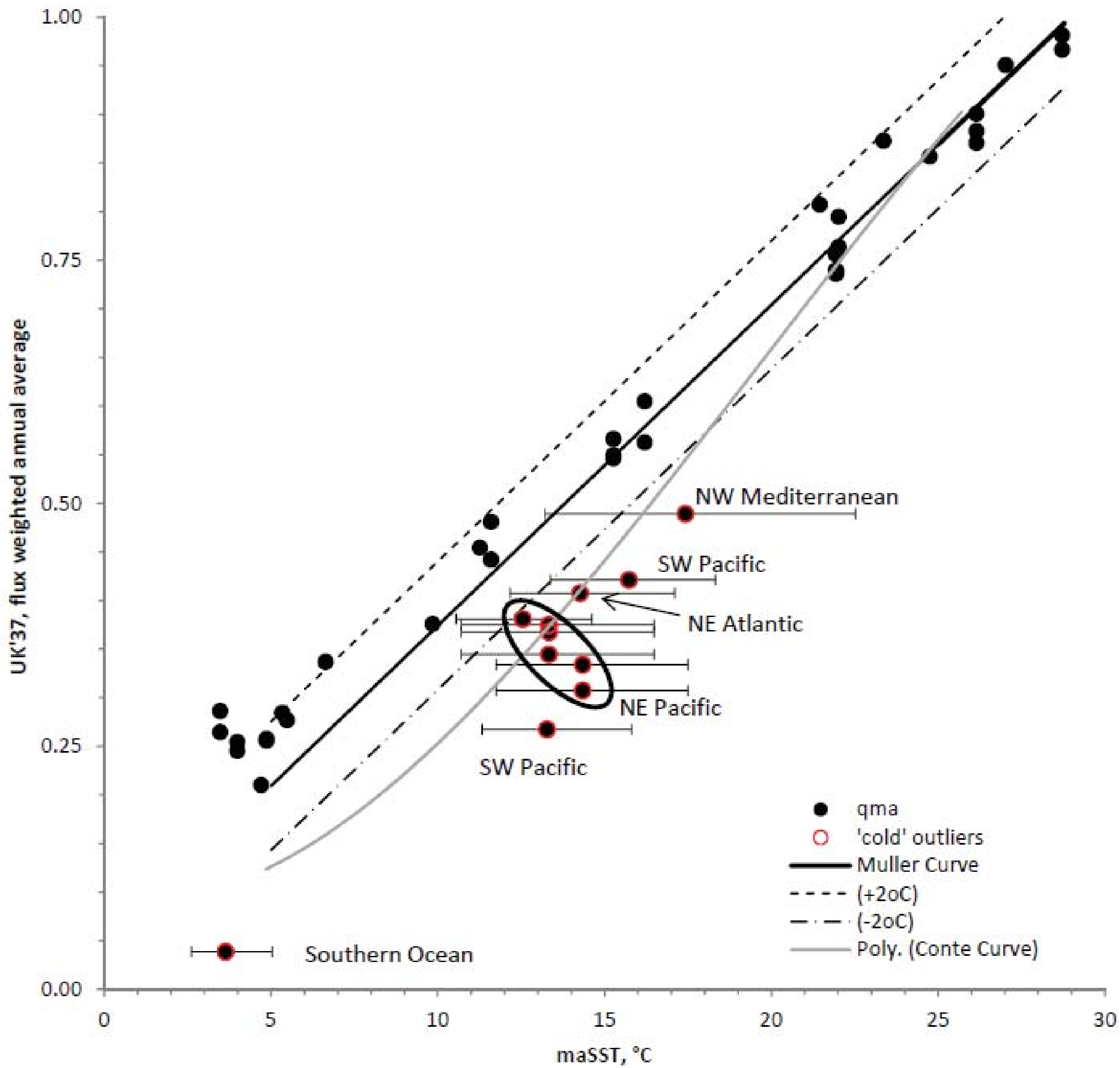

UK'37, flux weighted annual average
maSST, °C
NW Mediterranean
SW Pacific
NE Atlantic
NE Pacific
SW Pacific
Southern Ocean
qma
'cold' outliers
Muller Curve
(+2oC)
(-2oC)
Poly. (Conte Curve)

Figure 3B

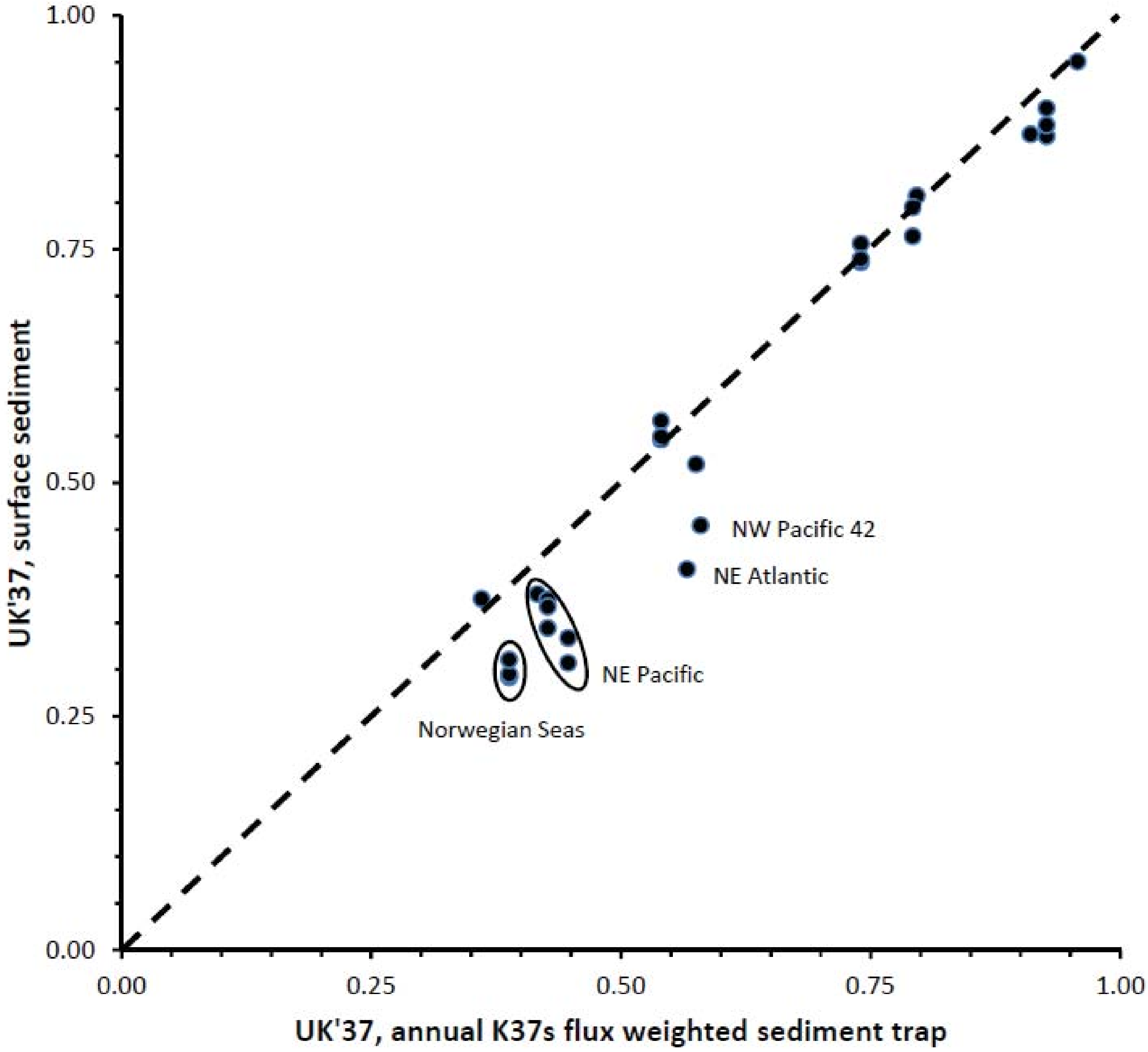

1.00
0.75
0.50
0.25
0.00
UK'37, surface sediment
NW Pacific 42
NE Atlantic
NE Pacific
Norwegian Seas
0.00
0.25
0.50
0.75
1.00
UK'37, annual K37s flux weighted sediment trap

Figure 4A

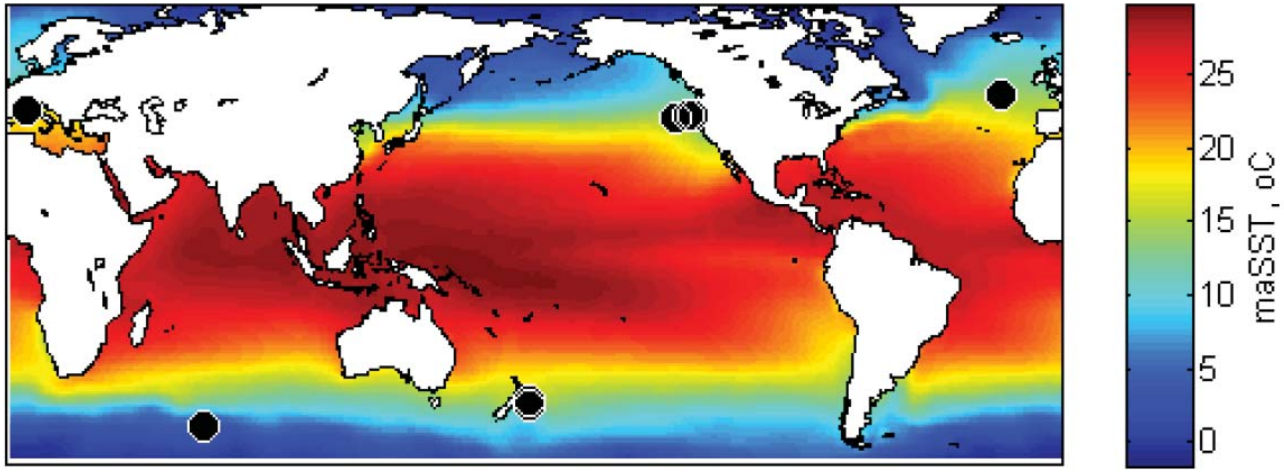

Figure 4B